Acta Geochim (2026) 45:30–41
https://doi.org/10.1007/s11631-025-00840-4

ORIGINAL ARTICLE

# Behavior of opaque minerals in the Jilin H5 chondrite experimentally shocked to 12–133 GPa pressures

**Xiande Xie[1,2] · Jiarui Lin[1,2] · Haiyang Xian[1,2]**

Received: 15 October 2025 / Revised: 5 November 2025 / Accepted: 24 November 2025 / Published online: 6 January 2026


**Abstract** Recovered samples of Jilin H5 chondrite experimentally shocked to 12–133 GPa were studied to explore the behavior of opaque minerals under shock loading using SEM–EDS, Raman spectroscopy, and TIMA. The following results were obtained. Firstly, at pressures lower than 53 GPa, the opaque minerals still keep the unmelted state, while at 78 GPa and higher, FeNi metal and troilite form eutectic intergrowths occurring as disorderly fine veinlets filling the shock-induced fractures in silicate minerals. Secondly, single kamacite grains still maintain their contour at 12 GPa, but a part of brittle troilite grains was fragmented and squeezed into the shock-induced fractures within kamacite grains. At 53 and 133 GPa, many more troilite fragments are poured in the kamacite interior to form disordered hybrid aggregates or to form squiggly strips, respectively. Similar phenomena are observed within single troilite grains, but the mineral squeezed into troilite grains is kamacite. Thirdly, chromite is a hard and refractory oxide mineral. When the shock pressure rises step by step from 12 to 133 GPa, the shock effect of chromite is only fragmentation. Its grain size decreases from tens of μm at 53 GPa to a few μm at 133 GPa. And, fourthly, native copper exhibits distinct redistribution behavior at high temperature. In Jilin samples shock-loaded to 12 GPa, copper initially located at troilite–kamacite interfaces partially transferred into small troilite grains containing fine FeNi particles. At 53 and 133 GPa, native copper preferentially transferred into larger troilite grains containing more particles of eutectic FeNi metal.

**Keywords** Jilin chondrite · Shock–recovery experiment · High-pressure · Metallic minerals · Shock effects

## 1 Introduction

Shock–recovery experiments on chondrites are an effective means of studying the behavior of minerals under extreme high pressures and high temperatures. Although the duration of the high-pressure regime of such experiments is very short, quite a lot of valuable information about the material composition, physical and chemical states, and P–T conditions of the deep Earth has been provided (Bogard et al. 1987; Dai et al. 1991; Miyahara et al. 2021; Schmitt and Stoffler 1995; Sears et al. 1984; Xie et al. 2000, 2001). However, most of these studies were concentrated on silicate minerals, mainly olivine, pyroxene, feldspar, and silicate melt. The studies of opaque minerals in experimentally shocked meteorites are quite rare. In our previous study on Jilin H5 chondrite experimentally shocked to 12–133 GPa, we also focused on silicate minerals and their high-pressure polymorphs (Xie et al. 2001). In order to compensate for these deficiencies, we recently conducted systematic research on the behavior of opaque minerals in recovered samples of Jilin chondrite experimentally shocked to 12–133 GPa using a modern micro-mineralogical technique. This paper reports the results of this study.

✉ Xiande Xie
xdxie@gzb.ac.cn

[1] State Key Laboratory of Deep Earth Processes and Resources, Guangzhou Institute of Geochemistry, Chinese Academy of Sciences, Guangzhou 510640, China

[2] Center for Advanced Planetary Science (CAPS), Guangzhou Institute of Geochemistry, Chinese Academy of Sciences, Guangzhou 510640, China

## 2 Samples and methods

Shock–recovery experiments were conducted by Dai et al. (1991) with a two-stage light-gas gun. Samples of Jilin meteorite were shock-loaded to peak pressures of 12, 27, 39, 53, 78, 93, and 133 GPa. After the experiments, the recovered samples were sectioned, polished, sealed in plastic containers, and stored in a desiccator to prevent humidity and oxidation. These well-preserved sections were used in this study.

Shock-loading experiments on the Jilin meteorite samples were performed on the dynamic high-pressure device equipped with a two-stage light gas gun ($\varphi$23 mm inner caliber). Experimental specimens were made into $\varphi$10 mm × 2 mm discs. Each specimen was pre-mounted in the recovery capsule to prevent direct contact between the flyer material or high-impedance material and the meteorite sample. Subsequently, the sample capsule was impacted by a hypervelocity flyer plate, generating a shock wave that propagated through the capsule to the meteorite sample (Dai et al. 1991). The sample assembly and the shock recovery fixture are plotted in Fig. 1. Various impedance flying plates and the two shock techniques were used to boost the shock pressure (Jing 1986). Lexan, Ly-12Al, and copper were used as flying plates. Copper and tungsten plates were used as high-impedance materials to reflect the shock wave. The impact velocity of the flying plates was measured by a magnetoflyer. The shock pressure was calculated by the impedance matching method, and the temperature and residual temperature were calculated by the thermodynamic formulae (Dai et al. 1991). The shock-loading conditions of the Jilin meteorite samples are listed in Table 1.

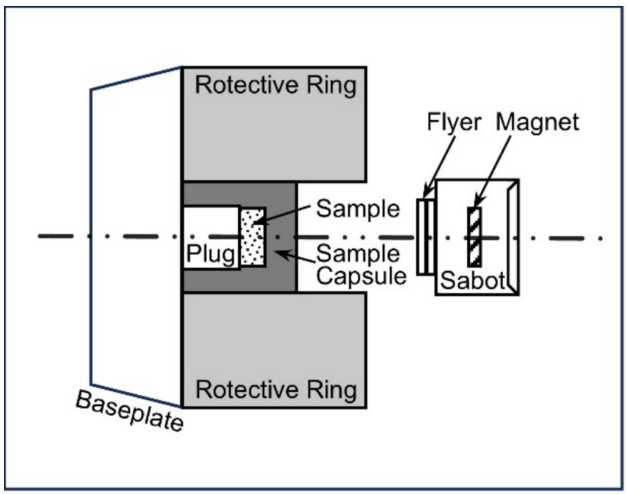


**Fig. 1** Scheme of sample assembly and the shock recovery fixture

The shock-recovered Jilin samples were analyzed using scanning electron microscopy (Thermo Fisher Scientific FEI Helios CX5) with energy dispersive spectroscopy (SEM–EDS), electron probe microanalysis (EPMA; CAMECA SX FE electron probe microanalyzer, Raman spectroscopy, and a texture and image-based mineral analysis (TIMA-X integrated mineral analyzer; TESCAN).

High-resolution mineral phase identification analysis was performed using the integrated mineral analyzer. Analytical conditions included a pixel spacing of 1.5 µm, 10,000 X-ray counts per pixel, a scanning speed of 50 µm/s, and an accelerating voltage of 25 kV with a beam current of 8.5 nA.

Microstructural observations of the minerals were conducted using SEM. Backscattered electron (BSE) images were acquired under an accelerating voltage of 10 kV and a beam current of 2.8 nA.

Raman spectra were acquired using a Renishaw in Via spectrometer with a 785-nm $Ar^+$ laser (1 mW) to avoid laser-induced thermal effects. Each spectrum was collected in step mode (0.5 s per step, 60 accumulations). After each acquisition, the sample was inspected to confirm the absence of laser ablation. Spectra were processed using WiRE 5.5 software for cosmic ray removal, baseline correction, and smoothing.

Quantitative chemical compositions of minerals were determined using EPMA. Analytical conditions were: 20 kV accelerating voltage, 20 nA beam current, and a

**Table 1** Shock-loading conditions of Jilin meteorite samples[a]

| No. of shoot | Impact velocity (km/s) | Shock pressure (GPa) | | Temperature (K) | | Flyer material | High-impedance material |
|---|---|---|---|---|---|---|---|
| | | Initial | Peak | Shock | Residual | | |
| 1 | 2.508 | 8.0 | 12 | 336 | 297 | Lexan | Cu |
| 2 | 2.258 | 18.2 | 27 | 472 | 386 | Ly-12 Al | Cu |
| 3 | 2.621 | 39.0 | 39 | 624 | 502 | Cu | / |
| 4 | 2.388 | 35.0 | 53 | 720 | 550 | Cu | W |
| 5 | 2.691 | 40.5 | 78 | 1120 | 832 | Cu | W |
| 6 | 3.066 | 48.2 | 93 | 1460 | 1064 | Cu | W |
| 7 | 3.927 | 68.5 | 133 | 2426 | 1725 | Cu | W |

[a]After Dai et al. (1991)

beam diameter of 1 μm (point mode for fine-grained minerals; nominal 0-μm setting corresponding to the minimum focused spot, ca. 1–2 μm in actual size).

## 3 Results

### 3.1 Occurrence of opaque minerals in unshock-loaded Jilin meteorite

The opaque minerals identified so far in the Jilin meteorite chiefly consist of FeNi metal (kamacite and taenite), troilite, and chromite. We also found some trace opaque minerals, such as native copper, ilmenite, sphalerite, and schreibersite. We were only able to study the behavior of FeNi metal, troilite, ilmenite, and native copper in the experimentally shocked Jilin samples, as the remaining opaque minerals occurred in extremely small amounts.

Kamacite occurs mostly as irregular grains or aggregate, packing interstitially in the crystal grains of silicate minerals olivine and pyroxene (Fig. 2a). Most kamacite grains are smaller than 1 mm in size, but the largest grains can reach 1.8 × 2.0 mm in diameter. The chemical composition of kamacite (average of 5 analyses, in wt%) is: Fe–93.13, Ni–6.25, Co–0.48, Zn–0.03, Cu–0.02, total–99.89. The distribution of Ni in kamacite seems to be very uniform.

Taenite largely occurs as granular grains distributed along margins of some kamacite grains (Fig. 2a), or as ribbons distributed within coarse-grained metallic phases. These two types of taenite exhibit distinct Fe/Ni ratios, namely $Fe_2Ni(Co)$ for the granular form and FeNi(Co) for the ribbon form. The former, varying from 10 to 200 μm in diameter with the composition of (average of 5 analyses, in wt%) Fe–67.26, Ni–31.60, Co–0.15, Cu–0.16, total–99.25, and the latter (ribbon occurrence) has the width by length of ribbons to be (10–30) × (50–150) μm, and with the composition of Fe–51.12226, Ni–46.2137, Co–0.08, Zn–0.02, Cu–0.28, total–97.77, respectively.

Troilite in the Jilin meteorite is mainly distributed in the matrix and tends to form closely packed mosaic

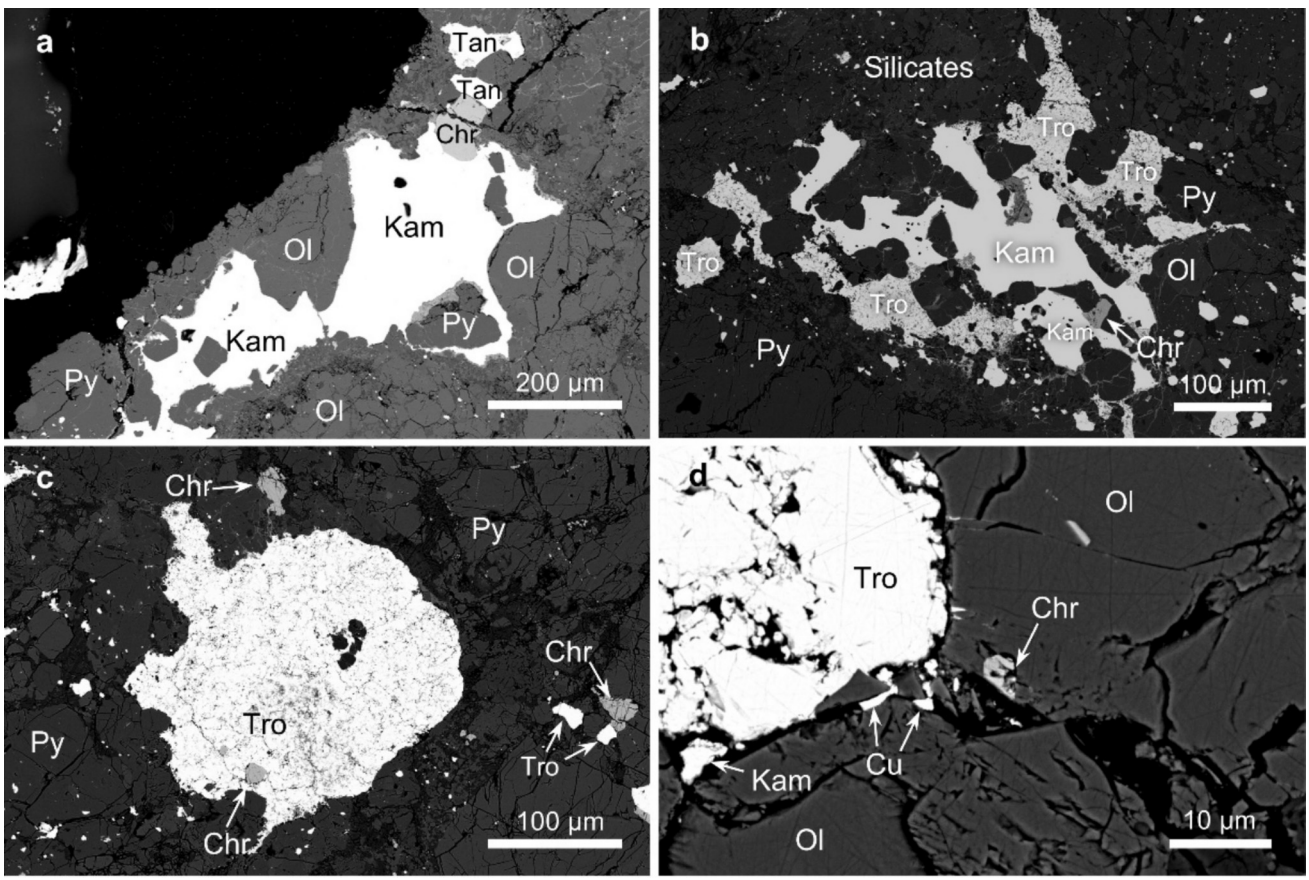


**Fig. 2** BSE images showing the occurrence of opaque minerals in the Jilin H5 chondrite: ***a*** a kamacite (*Kam*) grain is connected with smaller grains of taenite (*Tan*) and chromite (*Chr*); ***b*** troilite (*Tro*) grains are mainly distributed in the matrix and tend to form closely packed mosaic aggregates with Kam; ***c*** a troilite grain with unsmooth surface contains a chromite inclusion; and ***d*** two native copper grains are observed at the troilite–silicate interface. *Py* pyroxene, *Ol* olivine

aggregates together with kamacite (Fig. 2b), or serves as filling material in the space between transparent mineral grains (Fig. 2c) or within the fractures. The chemical composition of troilite seems relatively constant and the EPMA analyses gave the following results (average of 5 analyses, in wt%): Fe–62.56, Ni–0.24, Co–0.01, S–36.08, total–98.96.

Chromite commonly occurs as euhedral to subhedral crystals embedded in kamacite (Fig. 2a) and troilite (Fig. 2c) with grain sizes from 10 to 200 μm. A small number of chromite crystals is present in the interstices between metallic and transparent mineral grains or in the space between the transparent mineral grains (Fig. 2d). The EPMA analysis gave the following results (in wt%): FeO–28.96, MgO–2.83, MnO–0.67, $TiO_2$–2.09, $Cr_2O_3$–55.39, $Al_2O_3$–6.37, $V_2O_5$–0.70, total–97.48.

Native copper is extremely rare in the Jilin meteorite, with only two irregularly shaped grains (< 5 μm in diameter) observed at a fracture between troilite, kamacite, and olivine (Fig. 2d). In most cases, copper occurs as a trace element within kamacite, particularly concentrated along its serrated grain boundaries (Fig. 3). We could not obtain EPMA data for the native copper grains due to their small size.

### 3.2 General appearance of FeNi metal and troilite in the Jilin shock-loaded samples

The general pictures of FeNi metal and troilite in the Jilin meteorite experimentally shocked to 12–133 GPa are shown in Fig. 4. Owing to the shock temperatures in the samples shock-loaded below 53 GPa (Table 1) being lower than the melting points of iron (1538 ºC), Ni (1453 ºC), and FeS (1194 ºC), the opaque minerals in these samples still keep the unmelted state, although their shapes and grain sizes are different. Such phenomena are clearly showed in Fig. 4a–e. However, in the samples shock-loaded at 78 GPa and higher, we see a big change in the appearance of these two minerals (Fig. 4f–h). Except for a few larger grains, most of them occur as disorderly fine eutectic veinlets filling shock-induced fractures in silicate minerals. The thickness of veinlets is varying in a range of 1 to 5 μm, but, for some thick veinlets, it can reach 10 μm. At 78 GPa, the veinlets are

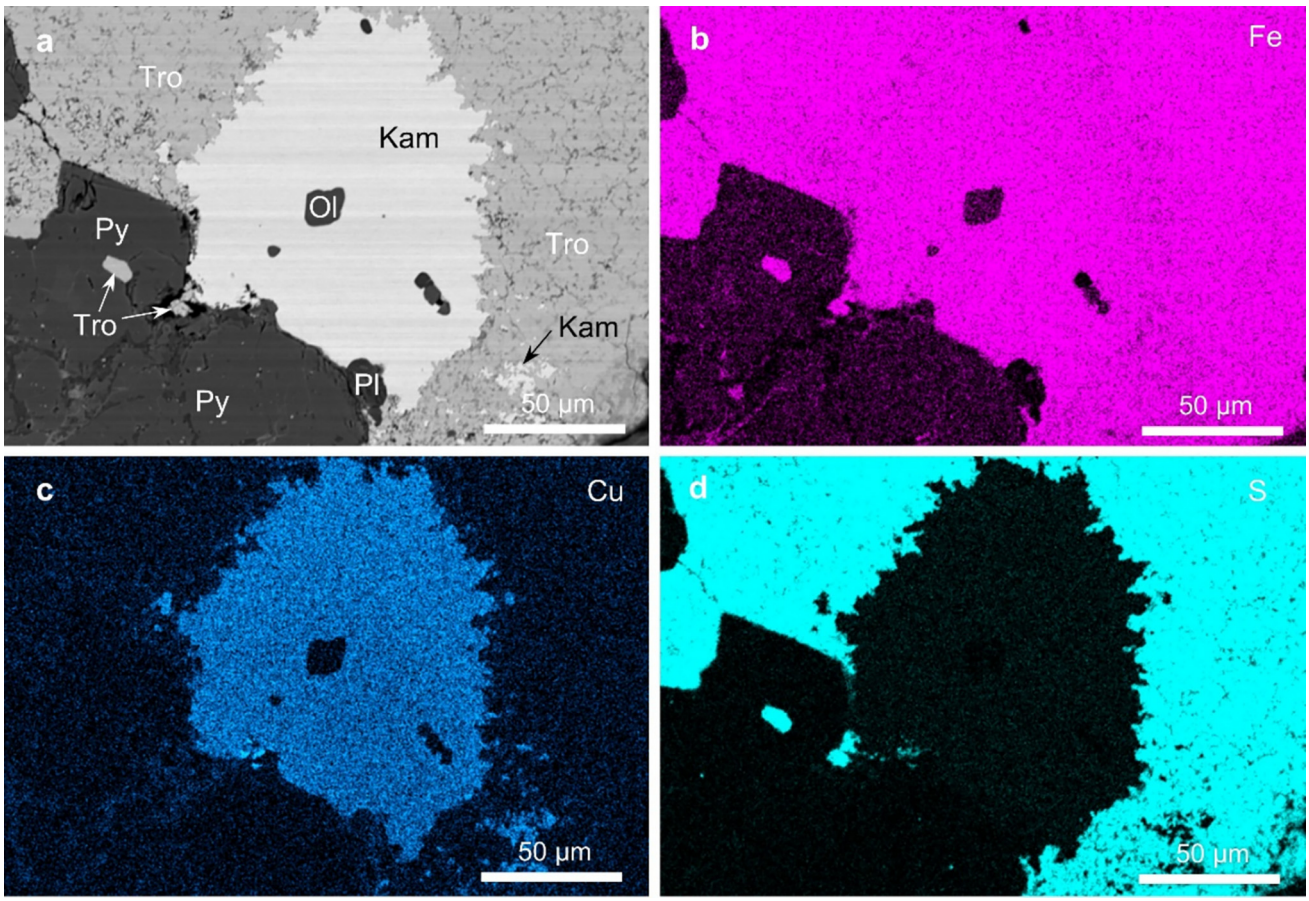


**Fig. 3** BSE images and EDS maps of Fe, Cu, and S from opaque minerals in the Jilin H5 chondrite. *Kam* kamacite, *Ol* olivine, *Pl* plagioclase, *Py* pyroxene, *Tro* troilite

thin and rather sparse, but, at 93 GPa, the veinlets become thinner and shorter but much denser. At 133 GPa, the shock temperature is very high and the veinlets begin to show some potential of aggregation to form irregular or strip-shaped grains and particles (Fig. 4h).

In order to reveal the nature of the opaque veinlets, we conducted EDS mapping of elements Fe, Ni, and S for the veinlets occurring in a pyroxene grain within the Jilin meteorite sample shock-loaded to 133 GPa (Fig. 5). The obtained maps clearly show that these opaque veinlets consist of FeNi metal and FeS, e.g., kamacite + taenite and troilite. Since the shock temperature in this shocked sample (1460 K or 1188 ºC; Table 1) is much higher than that for the formation of FeNi–FeS eutectics (988 ºC), we assume that these veinlets must consist of FeNi metal, FeS, or their eutectic mixtures. Figure 5e, f shows a thick FeNi–FeS eutectic veinlet of 8 μm in width filling a fracture in a shock-fractured pyroxene grain. This veinlet consists of numerous white-colored tiny rounded or elongated FeNi metal particles and the gray-colored FeS ground mass.

### 3.3 Behavior of single kamacite and taenite grains in shock-loaded samples of Jilin meteorite

The Jilin shock-loaded samples showed obvious shock effects in single kamacite and taenite grains. Since the taenite in the Jilin meteorite occurs in close contact with kamacite, and the content of taenite is much smaller than kamacite, and their main constituent elements are the same (Fe and Ni), we just use kamacite as the representative of these two FeNi minerals.

At 12 GPa, most of single kamacite grains still maintain their contour and smooth surface (Fig. 6a), but a part of the brittle troilite grains were fragmented and squeezed into the shock-produced fractures within tenacious kamacite grains (Fig. 6b). At 53 GPa, the single kamacite grains show corrosion borders, and many more troilite fragments are poured in the kamacide interior to form disordered hybrid aggregates (Fig. 6c, d). According to the phase diagram, the FeNi and FeS will form a eutectic mixture at the temperature of ≥ 988 ºC (Villars et al. 1995)**.** The shock temperature (2436 K or 2164 ºC) at 133 GPa is much higher than the melting points of Fe, Ni, and FeS, and the troilite fragments and aggregates at this condition would be further fused within the hot molten kamacite grains to form squiggly strips (Fig 6e, f).

### 3.4 Behavior of single troilite grains in shock-loaded samples of Jilin meteorite

The Jilin shock-loaded samples also show obvious shock effects in single troilite grains. At 12 GPa, single troilite grains still maintain their contour, but abundant shock-produced fractures are developed within them (Fig. 7a), and a few irregular kamacite grains were squeezed into some troilite grains along shock-induced fractures (Fig. 7b). At 53 GPa, the single troilite grains show corrosion borders, and many more kamacite fragments are poured into the troilite interior to form disordered hybrid aggregates of these two minerals (Fig. 7c, d). At 133 GPa, the kamacite fragments would be further fused within the hot molten troilite grains to form squiggly aggregates or irregular-shapes particles (Fig. 7e, f).

We conducted Raman spectroscopic analysis on the troilite in the shock-loaded samples of the Jilin meteorite (Fig. 8a), and it was revealed that the troilite in the unshock-loaded Jilin sample (0 GPa) shows typical Raman vibration peaks of Fe-S at 148, 197, and 308 $cm^{-1}$. Troilite in the sample shocked at 12 GPa gives similar Raman peaks to that of the unshocked sample., indicating that the crystal structure of troilite does not show an obvious change when the sample is shocked to pressures lower than 12 GPa. The Raman spectra of troilite in the samples shocked to 27–83 GPa showed notable changed in the drifting of the peak position and the weakening of signals, which might be caused by shock-induced lattice distortion and thermal disturbance. The Raman spectra of troilite in the samples shocked to 93 and 133 GPa become rather flat and more cluttered, indicating that the crystal lattice of troilite has been severely damaged or even decrystallized. At the same time, the appearance of weak Raman peaks of magnetite at 666 and 540 $cm^{-1}$ implies that, under such extremely high *P–T* conditions, troilite may experience some loss of S and oxidation of Fe to form secondary mineral magnetite during the decompression process.

### 3.5 Behavior of chromite in shock-loaded samples of Jilin meteorite

Chromite is a hard and refractory oxide mineral with its melting point at 1857 ºC. It has a cubic spinel structure and the oxygen ions exhibits cubic close-packing. Chromite in the unshocked Jilin meteorite occurs as single euhedral and subhedral grains of 10 μm in size. Owing to its hard and refractory characteristics, as well as its close-packing structure, the behavior of chromite in the shock-loaded samples of Jilin meteorite is rather simple. When the shock pressure rises step by step from 12 to 133 GPa, the shock effects of chromite mainly present as a continuous increase of the degree of fragmentation. For instance, the size of broken chromite fragments in the sample shocked to 53 GPa varies in the range of 50 to 100 μm, while that in the sample shocked to 133 GPa is reduced to 1 to 10 μm (Fig. 9).

The Raman spectra of chromite with typical peaks at 496, 598, and 688 $cm^{-1}$ in the Jilin samples shock-loaded to 12–133 GPa are shown in Fig. 8b, and it can be seen that all the Raman spectra of these samples look very similar despite

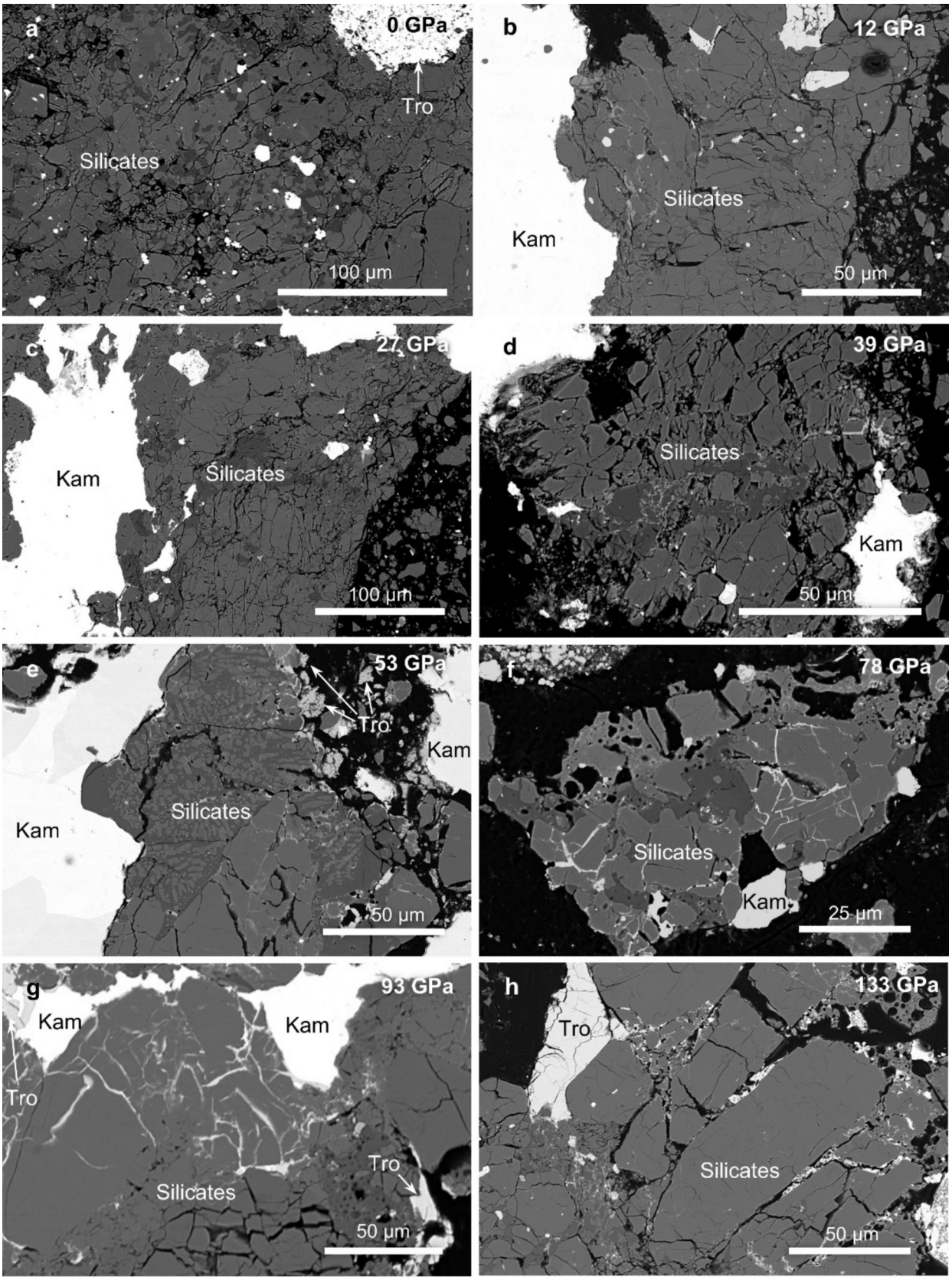
a
0 GPa
Tro
Silicates
100 μm
b
12 GPa
Silicates
Kam
50 μm
c
27 GPa
Kam
Silicates
100 μm
d
39 GPa
Silicates
Kam
50 μm
e
53 GPa
Tro
Kam
Kam
Silicates
50 μm
f
78 GPa
Silicates
Kam
25 μm
g
93 GPa
Kam
Kam
Tro
Tro
Silicates
50 μm
h
133 GPa
Tro
Silicates
50 μm

◂**Fig. 4** BSE images of a set of shock-loaded samples of Jilin meteorite showing the formation and evolution of opaque veinlets at pressures higher than 53 GPa: ***a–e*** The opaque minerals still keep the unmelted state, although their shapes and grain sizes are differ; ***f*** the opaque minerals appear in the form of fine veinlets filling the fractures in silicate minerals; ***g*** the veinlets become more thinner and much denser; ***h*** The veinlets begin to show some potential of aggregation to form irregular or strip-shaped grains and particles

the differences in pressure that they experienced being quite large. A small change can be noticed only in the slight drifting of the peak position and the weakening of signals at 496 and 598 $cm^{-1}$ for the chromite in the samples shock-loaded to 93 and 133 GPa, respectively.

### 3.6 Behavior of native cooper in shock-loaded samples of Jilin meteorite

Copper possesses very strong chalcophile properties, but, under the conditions found in meteorites, its behavior is like that of siderophile elements (Xie et al. 2024). It was found that troilite may be the primary carrier of copper in meteorites, but taenite is another important carrier phase (Łuszczek

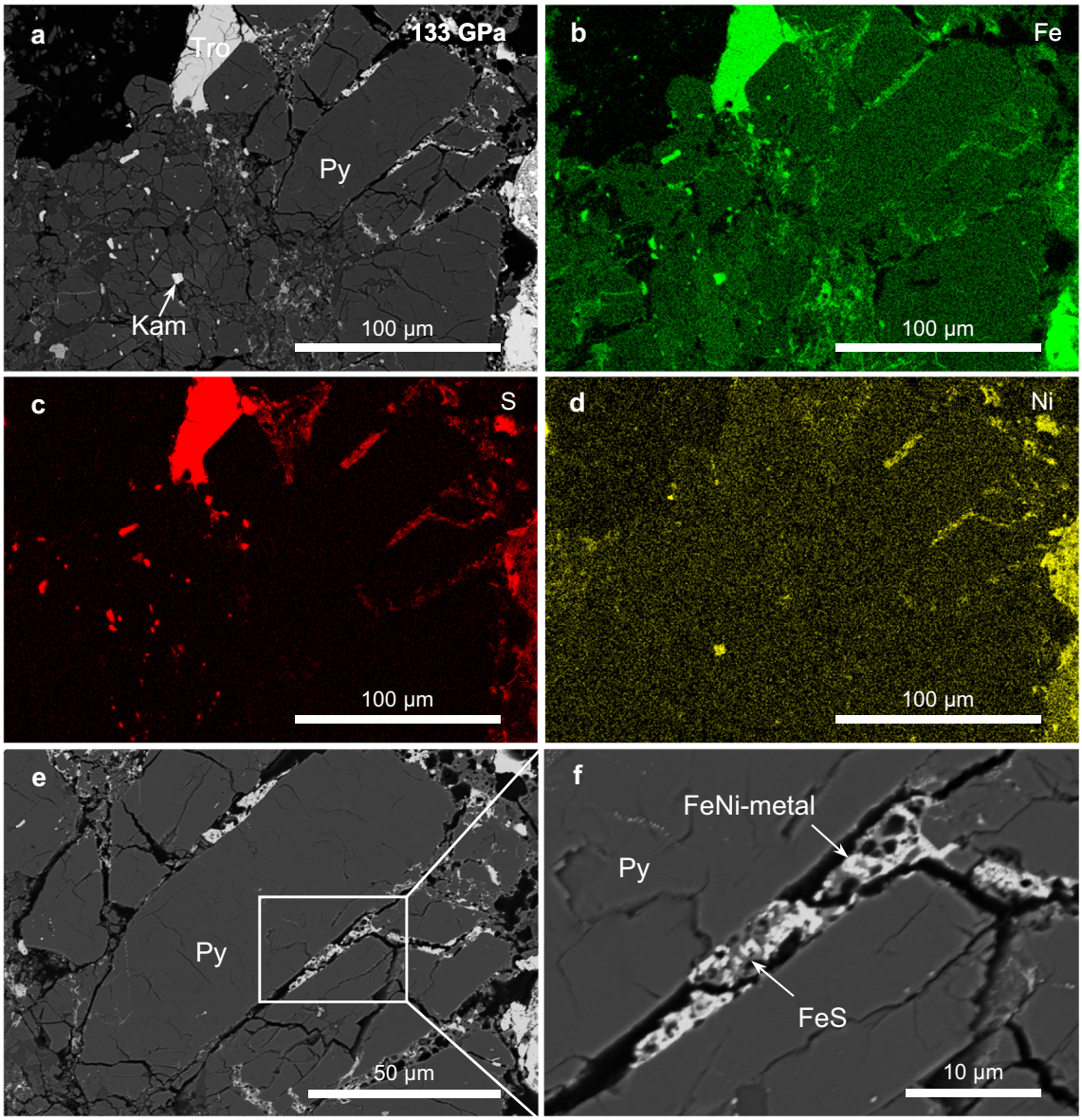


**Fig. 5** BSE images and corresponding EDS maps of Fe, S, and Ni taken from a Jilin sample shock-loaded to 133 GPa: ***a–d*** BSE images and Fe, S, and Ni maps showing fine vein-like intergrowths of troilite (*Tro*) and kamacite (*Kam*) within pyroxene (*Py*) fractures. ***e***, ***f*** magnified BSE images of the FeNi–FeS eutectic vein in (***a***). Note the numerous white-colored tiny rounded or elongated FeNi metal particles dispersed in the gray-colored FeS ground mass

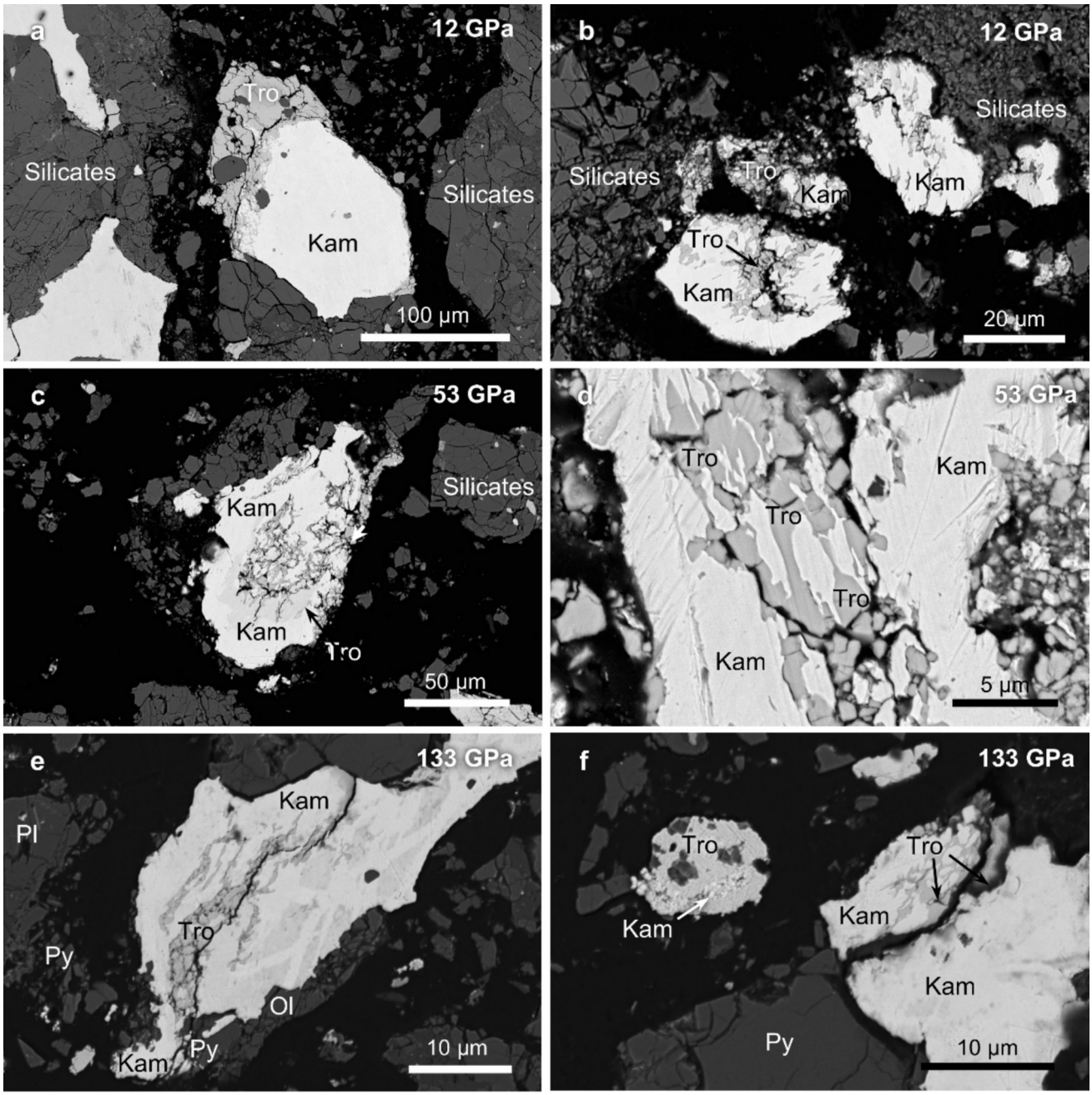


**Fig. 6** BSE images of Jilin shock-loaded samples showing the shock effects in kamacite: ***a***, ***b*** at 12 GPa, single kamacite grains still maintain their contour, but a part of the brittle troilite grains were fragmented and squeezed into the shock-induced fractures within kamacite grains; ***c***, ***d*** at 53 GPa, the single kamacite grains show corrosion borders, and many more troilite fragments are poured in the kamacide interior to form disordered hybrid aggregates; ***e***, ***f*** at 133 GPa, the troilite fragments and aggregates would be further fused within the hot molten kamacite grains to form squiggly strips

and Krzesińska 2020), It was also revealed that, during natural shock events, copper could become redistributed in meteorites; namely, copper is transferred into the intergrowths of FeNi metal and troilite (Xie et al. 2024). Such a phenomenon has also been observed in the Jilin meteorite samples experimentally shocked to 12–133 GPa (Fig. 10).

Native copper has melting point (1083 ºC) much lower than kamacite and troilite, and it diffuses easily at high temperatures. Hence, in the Jilin sample shock-loaded to 12 GPa, some diffused copper is transferred into small troilite grains containing some tiny particles of FeNi metal (Fig. 10c, d). When the pressure rises to 53 and 133 GPa, native copper disappears and the released Cu is transferred into larger

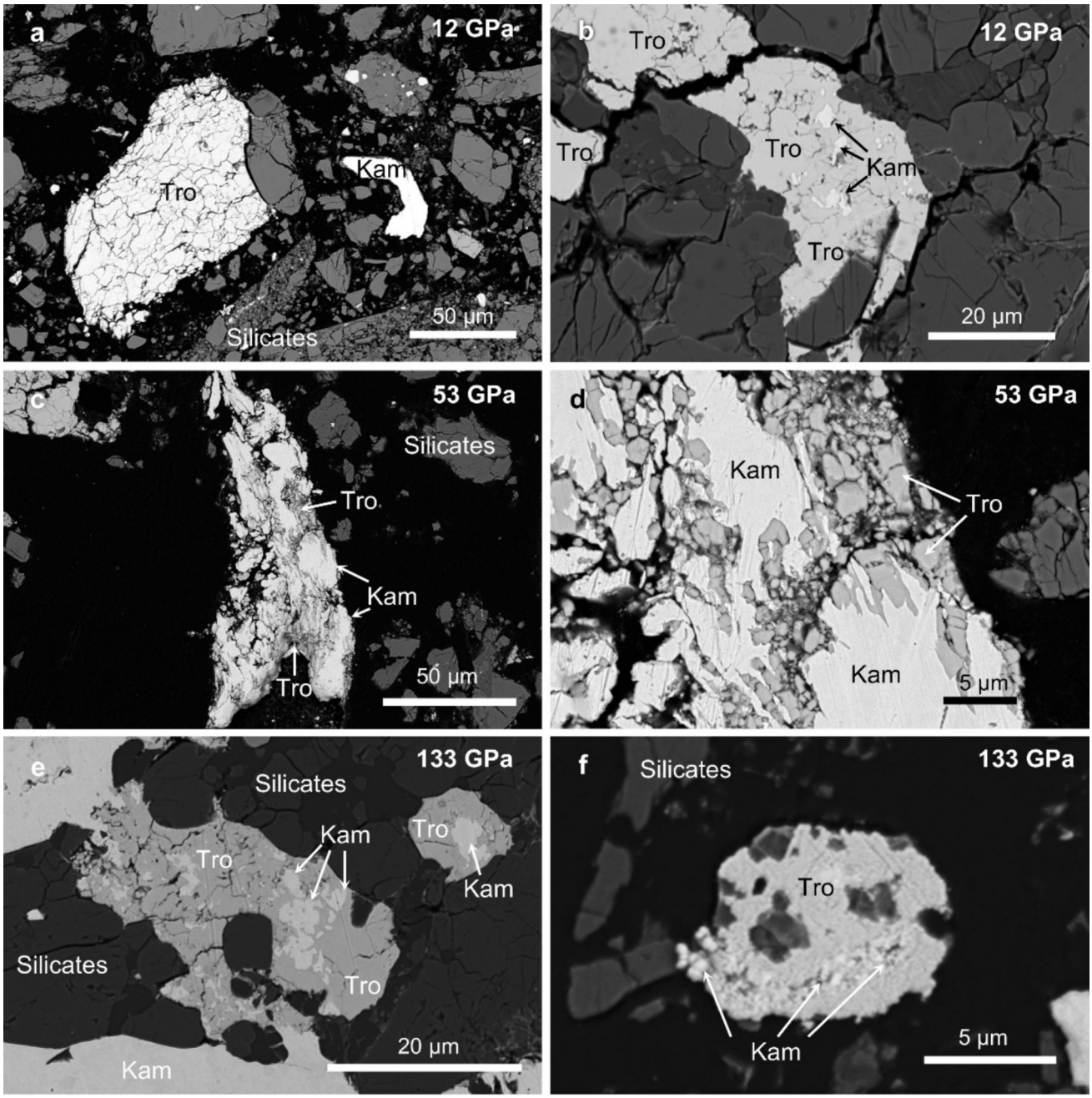


**Fig. 7** BSE images of Jilin shock-loaded samples showing the shock effects in troilite: ***a***, ***b*** At 12 GPa, troilite grains still maintain their contour, but abundant shock-produced fractures are developed within them, and a few of kamacite grains were squeezed into some fractures within troilite grains; ***c***, ***d*** at 53 GPa, the troilite grains show corrosion borders, and many more kamacite fragments are poured into the troilite interior to form disordered hybrid aggregates of these two minerals; ***e***, ***f*** at 133 GPa, the kamacite fragments would be further fused within the hot molten troilite grains to form squiggly aggregates or irregular-shaped particles

troilite grains (Fig. 10e–h). As the behavior of copper in experimentally shocked Jilin samples is more complicated and quite interesting, the detailed description of the result of our study on this issue will be published in another paper.

## 4 Conclusions

1. At pressures lower than 53 GPa, the opaque minerals still keep the unmelted state, while, at 78 GPa and

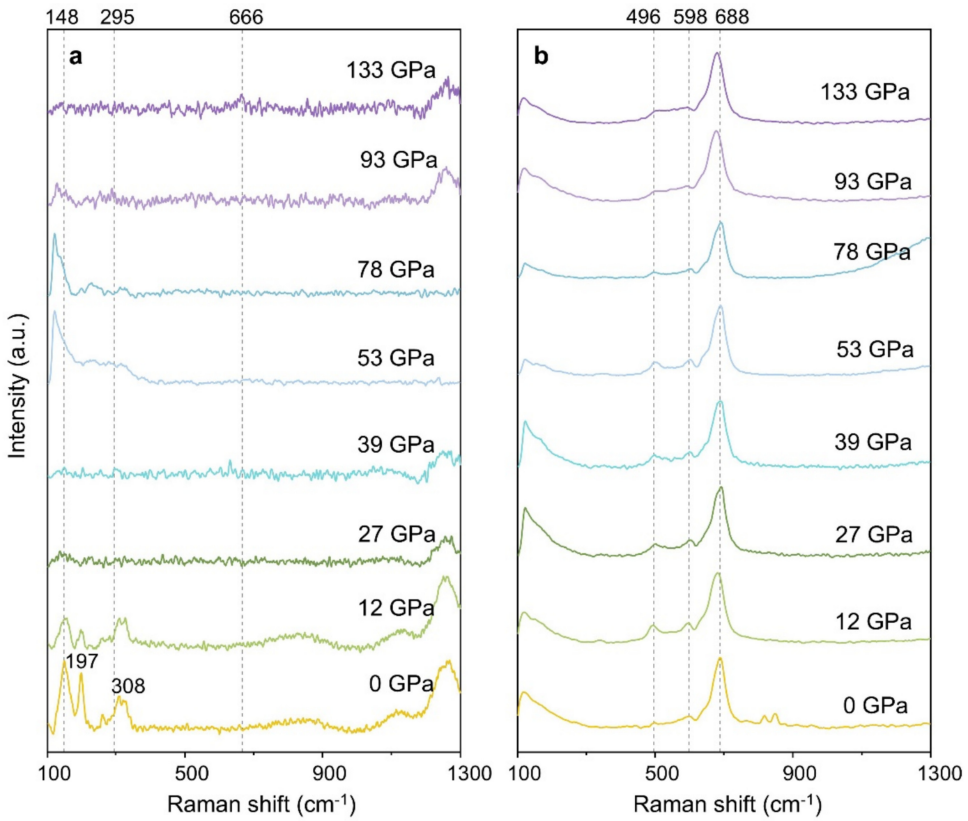


**Fig. 8** Raman spectra of troilite (***a***) and chromite (***b***) in the shock-loaded Jilin meteorite samples

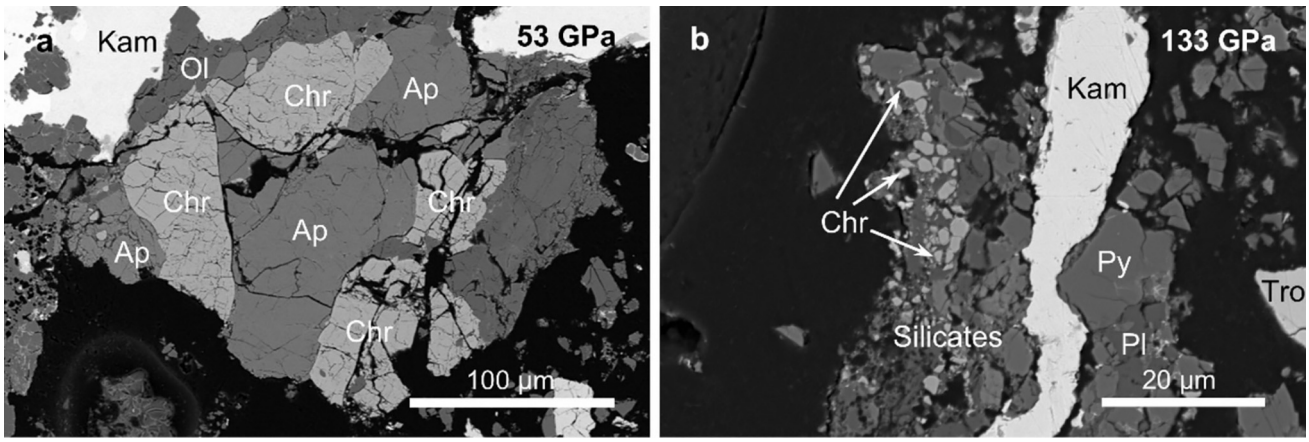


**Fig. 9** BSE image of Jilin shock-loaded Jilin samples showing the shock effects in chromite; *Ap* apatite, *Chr* chromite, *Kam* kamacite, *Ol* olivine, *Pl* plagioclase, *Py* pyroxene, *Tro* troilite

higher, FeNi metal and troilite form eutectic intergrowths appearing as fine, disordered veinlets that fill shock-induced fractures in silicate minerals.

2. Single kamacite and troilite grains still maintain their contour at 12 GPa, although some brittle troilite grains are fragmented and squeezed into shock-induced fractures within the kamacite. At 53 GPa, many more troilite fragments are poured in the kamacite interior to form disordered hybrid aggregates. At 133 GPa, the troilite fragments and aggregates would be further fused within the hot molten kamacite grains to form squiggly strips. Similar phenomena are observed within single troilite grains, but the mineral squeezed into troilite grains is kamacite.
3. Chromite is a hard and refractory oxide mineral. When the shock pressure rises step by step from 12 to 133 GPa,

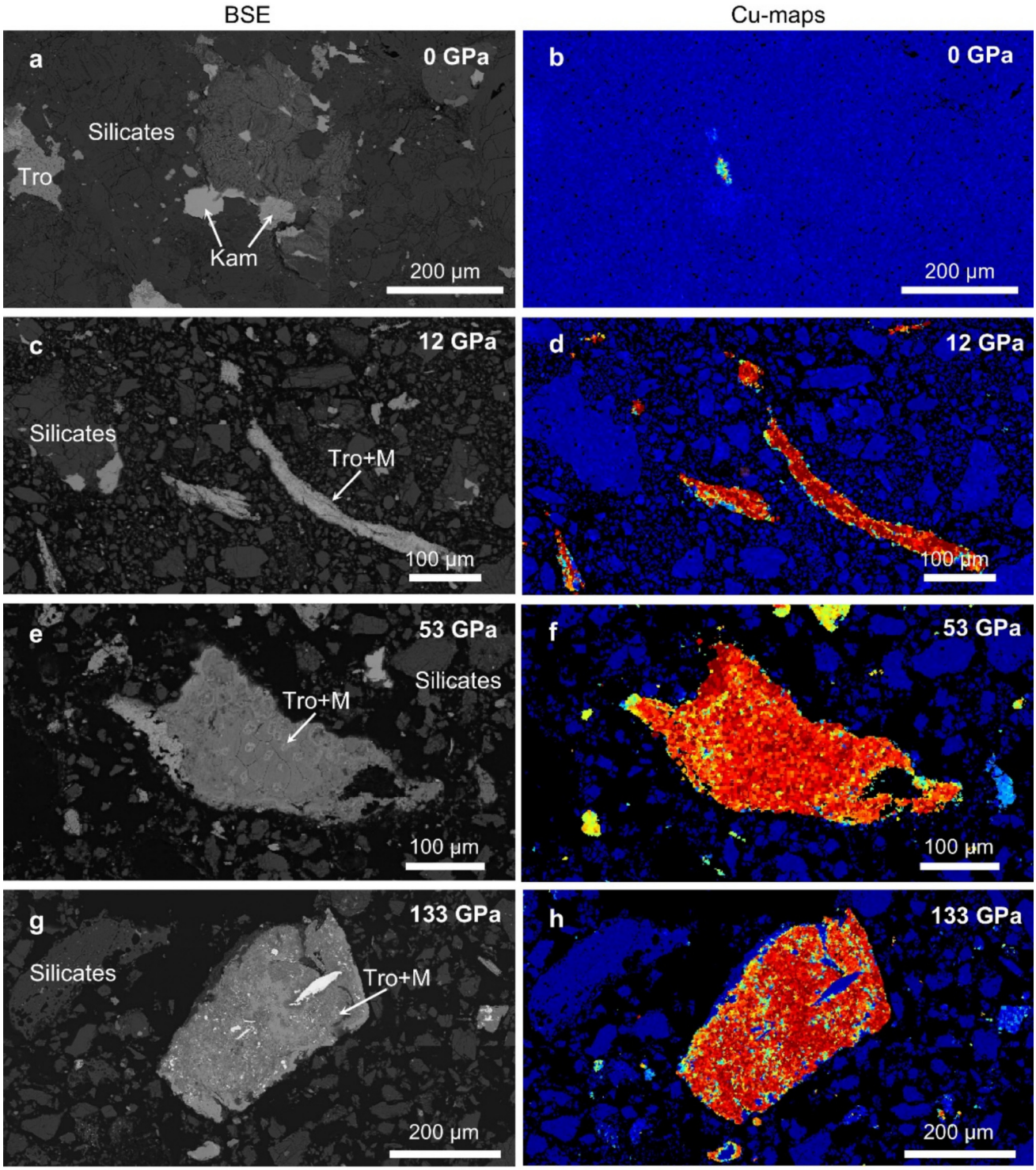


**Fig. 10** BSE images and Cu maps showing the redistribution of copper in Jilin samples shock-loaded to: (**a**, **b**) 0 GPa, (c, d) 12 GPa, (**e, f**) 53 GPa, and (**g, h**) 133 GPa. Note that the content of eutectic FeNi metal particles in troilite grains is increasing with the increasing of shock pressures. In the Cu maps, the concentrations of Cu in are higher than those in *yellow*. Tro + M Troilite + eutectic FeNi metal

the shock effect in chromite is only fragmentation. Its grain size decreases from tens of um at 53 GPa to a few μm at 133 GPa.

4. Native copper has a melting point much lower than that of kamacite and troilite. Its mode of occurrence undergoes notable changes at high temperatures. Hence, in

the Jilin sample shock-loaded to 12 GPa, native copper originally located at the troilite edges or within the kamacite partially transferred into small troilite grains containing some tiny particles of FeNi metal. At 53 and 133 GPa, native copper preferentially transferred into larger troilite grains containing more particles of eutectic FeNi metal.

**Acknowledgements** This research is supported by Science and Technology Planning Project of Guangdong Province, 2023B1212060048. We are grateful to P.L. He for assistance with EPMA analysis, to M.M. Zhang for assistance with Raman spectroscopy analysis, and to C.Y. Zhao for assistance with scanning electron microscopy analysis.

**Author contributions** Xiande Xie: research project design and implementation, reflective microscopy observation of minerals, image production, and writing the initial draft of the paper; Jiarui Lin: scanning electron microscopy with energy dispersive spectroscopy, electron probe microanalysis, Raman spectroscopy, participating in the discussion of the initial draft of the paper; Haiyang Xian: responsible for high-resolution mineral phase identification analysis using a TIMA-X integrated mineral analyzer, and participating in the discussion of the initial draft of the paper.

**Funding** Science and Technology Planning Project of Guangdong Province,2023B1212060048, Xiande Xie.

**Declarations**

**Conflict of interest** The authors declare that they do not have any known competing financial interests or personal relationships that could have appeared to influence the work reported in this paper.

## References

Bogard D, Hörz F, Johnson P (1987) Shock effects and argon loss in samples of the leedey l6 chondrite experimentally shocked to 29–70 GA pressures. Geochim Cosmochim Acta 51(7):2035–2044. https://doi.org/10.1016/0016-7037(87)90192-x

Dai CD, Wang DD, Jin XG (1991) A shock-loading experimental study of Jilin meteorite samples. Chin Sci Bull 36(23):25–32

Jing F (1986) Introduction to experimental equation of state. Introduction to Experimental Equation of State. Science Press, Beijing, pp 320–323

Łuszczek K, Krzesińska AM (2020) Copper in ordinary chondrites: proxies for resource potential of asteroids and constraints for minimum-invasive and economically efficient exploitation. Planet Space Sci 194:105092. https://doi.org/10.1016/j.pss.2020.105092

Miyahara M, Tomioka N, Bindi L (2021) Natural and experimental high-pressure, shock-produced terrestrial and extraterrestrial materials. Prog Earth Planet Sci 8(1):59. https://doi.org/10.1186/s40645-021-00451-6

Schmitt R, Stoffler D (1995) Experimental data in support of the 1991 shock classification of chondrites. Meteoritics 574–575.

Sears DW, Ashworth JR, Broadbent CP, Bevan AWR (1984) Studies of an artificially shock-loaded H group chondrite. Geochim Cosmochim Acta 48(2):343–360. https://doi.org/10.1016/0016-7037(84)90255-2

Villars P, Prince A, Okamoto H (1995) Handbook of ternary alloy phase diagrams. Cu-Mg-Si to Ga-Hg-Te. ASM International

Xie XD, Chen M, Dai CD, El Goresy A (2000) Characteristics in naturally and experimentally shocked chondrites: a clue to P-T conditions of impacted asteroids. Sci China Ser D Earth Sci 43(5):480–486. https://doi.org/10.1007/BF02875309

Xie XD, Chen M, Dai CD, El Goresy A, Gillet P (2001) A comparative study of naturally and experimentally shocked chondrites. Earth Planet Sci Lett 187(3–4):345–356. https://doi.org/10.1016/s0012-821x(01)00297-7

Xie XD, Gu XP, Yang YP (2024) The occurrence of metallic copper and redistribution of copper in the shocked Suizhou L6 chondrite. Acta Geochim 43(5):827–837. https://doi.org/10.1007/s11631-024-00703-4